

High-resolution IR spectra of the ozone molecule

S.N. Mikhailenko,¹ A. Barbe,² V.I.G. Tyuterev,² and A. Chichery²

¹ *Institute of Atmospheric Optics,*

Siberian Branch of the Russian Academy of Sciences, Tomsk, Russia

² *Groupe de Spectrométrie Moléculaire et Atmosphérique de l'Université de Reims, France*

Received July 8, 1999

This paper summarizes the studies of the IR absorption spectra of the main isotopic specie of ozone in the region from microwave to 5800 cm^{-1} . The emphasis is on more recent papers which results are yet not included in the databases of spectroscopic information, such as GEISA and HITRAN. These papers mainly consider absorption bands in the region higher than 3500 cm^{-1} and weak bands in different spectral regions. All bands with $\Delta v = 5$ and 6 studied up to date are described.

Introduction

Ozone is one of the most important components of the earth's atmosphere; it substantially determines the character of solar radiation absorption by the atmosphere. Being a strong absorber of solar radiation in various spectral regions (most intense absorption is observed at wavelengths less than 2900 \AA), ozone protects all living beings on the Earth against dangerous UV radiation. Ozone was discovered in 1785 by Dutch physicist M. Van Marum by its characteristic smell and the oxidizing properties of air after passage of an electric spark through it. In 1840 the ozone was produced by Schoenbein, and in the following 50 years its fundamental absorption bands in the visible and UV spectral regions have been detected. It took about a century after the production of the ozone to understand its role in the atmospheric processes, including climate formation. The first conference devoted to atmospheric ozone was held in Paris in 1929. Nowadays the ozone problems are widely discussed at all conferences devoted to the atmosphere and global climate. The interest in atmospheric ozone in recent years is caused, in particular, by the problem of "ozone holes," i.e., depletion of the ozone layer under the anthropogenic impact. Ozone in the atmosphere is concentrated mainly at the altitudes from 10 to 50 km.

Among various methods of ozone studies, the spectroscopic methods occupy a significant place. Let us mention two reviews in the Russian literature devoted to this subject. S.V. Ivanov and V.Ya. Panchenko¹ consider the history of development of the infrared (IR) and microwave (MW) ozone spectroscopy since the midnineteenth century till early 1990s. The review by I.M. Sizova² presents the data on electronic absorption spectra and structure of electronic energy states of ozone (it summarizes the ozone studies until 1991). In the both reviews the authors note the absence of systematic data on rotational structure of IR spectra in the region higher than 3500 cm^{-1} . Spectra in this region are associated with transitions to high-excited vibrational states. In this paper we try to systematize the results of original works devoted to study of high-

resolution IR spectra of ozone in the $3500\text{--}5800\text{ cm}^{-1}$ spectral region.

Peculiarities of the IR spectrum of ozone

The ozone molecule is a nonlinear triatomic molecule consisting of three oxygen atoms. The experimentally observed rovibrational spectra of ozone correspond to so-called open configuration of the molecule.² Isotopic species of the ozone include both symmetric molecules ($^{16}\text{n}_3$, $^{18}\text{n}_3$, $^{16}\text{n}^{18}\text{n}^{16}\text{n}$, and others) and the molecules with asymmetric equilibrium configuration ($^{16}\text{n}^{16}\text{n}^{18}\text{n}$, $^{16}\text{n}^{18}\text{n}^{18}\text{n}$, $^{16}\text{n}^{17}\text{n}^{18}\text{n}$, and others). The symmetric isotopic modifications of the open configuration of ozone belong to the q_{2v} point symmetry group, whereas the asymmetric species belong to the C_s point group. The most abundant ozone specie under natural conditions is $^{16}\text{n}_3$ (99.2%) which is the main isotopic specie. Hereinafter in this paper, unless otherwise stated, our subject is the $^{16}\text{n}_3$ molecule and its absorption spectrum caused by transitions between rovibrational (RV) energy levels of the ground electronic state.

Ozone in its open configuration is an asymmetric top molecule. The rovibrational energy levels of this molecule are characterized by three vibrational ($v_1v_2v_3$) and three rotational J , K_a , K_c quantum numbers. In the q_{2v} symmetry group the symmetry of vibrational levels is uniquely determined by the number v_3 (even or odd). The vibrational bands with odd Δv_3 are usually called the A-type bands (v_3 , $v_1 + v_3$, $v_2 + v_3$, $3v_3$, etc.), whereas the bands with even Δv_3 are called the b-type bands (v_1 , v_2 , $2v_2$, $2v_3$, etc.). The statistical weights g_i of rovibrational energy levels of $^{16}\text{n}_3$ are equal to 0 and 1 for the symmetry types b_1 , b_2 and A_1 , A_2 , respectively (for the coordinate axes chosen in standard way¹). So, only transitions of the type $A_1 \leftrightarrow A_2$ are observed in the spectrum. The approximate relations between the frequencies of normal vibrations (Fig. 1) are the following:

$$\omega_1 \approx \omega_3 \quad (1a)$$

and

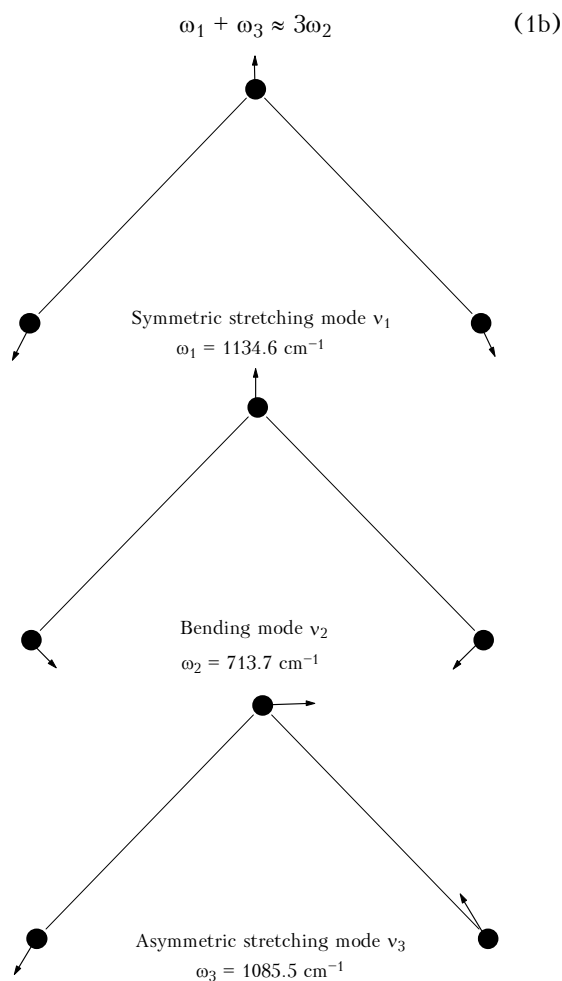


Fig. 1. Normal vibrational modes and harmonic frequencies of the $^{16}\text{n}_3$ molecule.

As a result, many vibrational levels are close to each other (on the energy scale) and the corresponding rotational–vibrational states are strongly interacting. The standard method for taking into account these interactions is constructing the effective rotational–vibrational Hamiltonians for polyads of interacting states. Most often such polyads incorporate a group of states with a fixed value of the quantum number v_2 and satisfying the condition

$$v_1 + v_3 = \text{const.} \quad (2)$$

Thus formed groups of states based only on the use of relation (1a) can be called "stretching polyads." So, the ground vibrational state (000) and the states (010) and (020) can be considered as isolated (Fig. 2b). The first groups of interacting states are the dyads $\{(100), (001)\}$ and $\{(110), (011)\}$ with the Coriolis resonance between the states. Next are the triads $\{(200), (101), (002)\}$ and $\{(210), (111), (012)\}$. The strong interaction between the states (200) and (002), (210) and (012) is called the Darling–Dennison resonance. This approach allows high-accurate description of the rotational structure of low vibrational states.^{3–10}

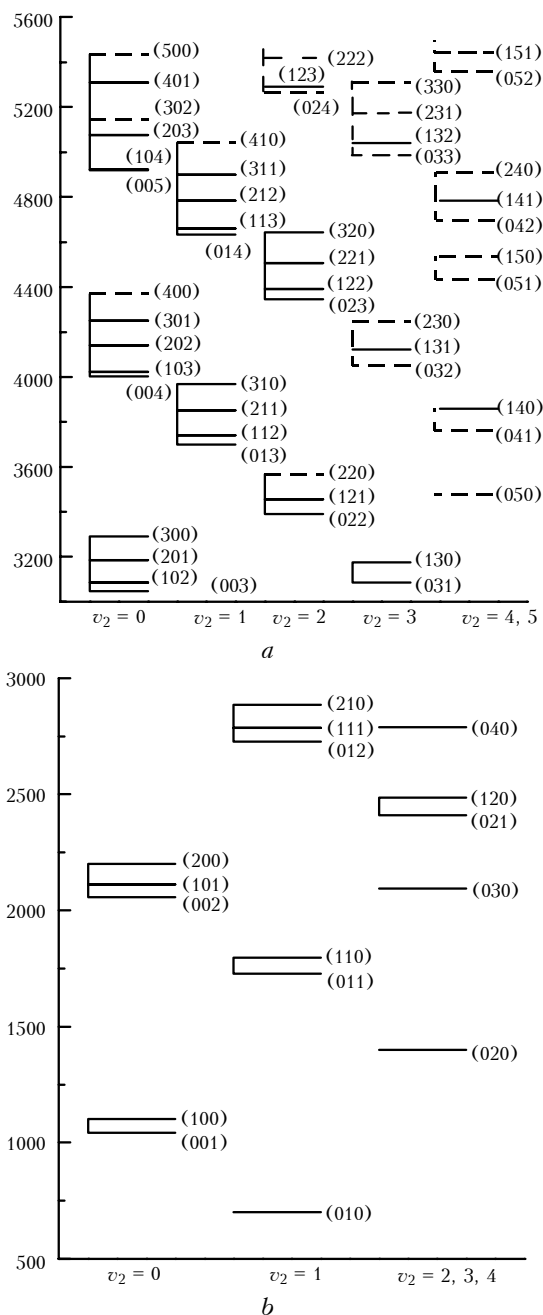


Fig. 2. Vibrational energy levels of the $^{16}\text{n}_3$ molecule in the energy ranges from 500 to 3000 cm^{-1} (b) and from 3000 to 5600 cm^{-1} (a).

Since ozone is a heavy molecule and the difference between the vibrational frequencies is not very large ($\approx 60 \text{ cm}^{-1}$ for ω_1 and ω_3), rovibrational energy levels are close to each other and can be divided into polyads according to Eq. (2), but this polyad structure clearly appear up to some energy only. Actually, the polyads corresponding to different quantum number v_2 begin to overlap starting already from the energy of 2000 cm^{-1} . For example, in Refs. 6 and 9 it is mentioned that the rotational structure of the states (101) and (201) is perturbed because of their interaction with the states

(030) and (130), respectively. This means that the rule of polyads formation should include both frequency relations (1a) and (1b). In this case, one polyad incorporates the vibrational states satisfying the condition

$$3\nu_1 + 2\nu_2 + 3\nu_3 = \text{const.} \quad (3)$$

In Refs. 11–13 to describe the rotational structure of the states (301), (212), and (203), the Coriolis interaction with the states (230), (141), and (132), respectively, was explicitly taken into account. Such resonance interactions between various vibrational states arise just due to relation (1b).

As seen in Fig. 2a, for energies above 3600 cm⁻¹ one can hardly separate out an isolated group of vibrational states. High density of vibrational states results in accidental coincidence of vibrational energies of various states not caused by the relations (1a) and (1b). On the other hand, energy distances among states entering into one polyad may be as large as 100 cm⁻¹ and even more. Because of these two circumstances, in practical processing of a spectrum one has to consider only a part of a polyad but include explicitly resonance interactions with states, formally belonging to other stretching polyads.^{14–17}

Most intense lines in the ozone spectrum correspond to rovibrational transitions with $\Delta K_a = 0$ and ± 1 . The probability of transitions with $|\Delta K_a| > 1$ and, consequently, the intensity of the corresponding lines for the asymmetric-top molecules very strongly depends on the degree of asymmetry of the inertia tensor of the molecule.¹⁸ It is commonly accepted to characterize this value by the parameter

$$\kappa = |(2b - A - q)/(A - q)|,$$

where A , b , and q are rotational constants of the molecule. The closer κ to unity, the weaker are the lines with $|\Delta K_a| > 1$. For the ozone molecule the value of κ exceeds 0.95, therefore the lines with $|\Delta K_a| > 1$ are observed only in the most intense bands, such as ν_3 , $\nu_1 + \nu_3$, ν_2 , and some others. For bands from the region higher than 3000 cm⁻¹ only the lines with $\Delta K_a = 0$ and ± 1 whose intensity most often does not exceed 10⁻²⁴ cm/mol are observable (under experimental conditions accessible to date). The apparent of lines with $|\Delta K_a| > 1$ in the spectrum, on the one hand, significantly simplifies the spectrum and facilitates its analysis and assignment. However, it also limits the number of transitions to the same upper level and thus often makes impossible an application of the method of combination differences to assign spectra.

The ozone molecule possesses a large moment of inertia, so its rotational constants are rather small. As a result, the rovibrational spectrum has high density of spectral lines (up to hundred lines) per one reciprocal centimeter. The density of lines is especially high in

R -branches of A-type bands (with odd Δv_3). A-type bands in the region higher than 3500 cm⁻¹ have a pronounced characteristic pattern. This pattern is caused by the compact and very dense R -branch with a sharp boundary at high frequencies and sufficiently long p -branch whose intensity drops gradually towards low frequencies. A typical A-type band is shown in Fig. 3a. As to the b-type bands, it is rather hard to separate the branches because they are extended and overlap each other as shown in Fig. 3b. The branches Q_P and Q_R are, as a rule, rather weak, what explains the dip at the center of a band (Fig. 3a). More intense band edges correspond to P_P -, P_R - and R_P -, R_R -branches.

Another consequence of small rotational constants and high density of RV energy levels is the fact that the maximum intensity of absorption bands corresponds to sufficiently high quantum numbers $J \approx 30$ –40. The maximum values of rotational quantum numbers for observed transition of strong bands range in the interval $J \approx 60$ –80 and $K_a \approx 15$ –25. In spite of so high rotational excitation of the molecule, non-rigidity effects are not very pronounced in ozone spectra. This explains the fact that nearly all ro-vibrational ozone lines of a band system corresponding to a given set of interacting states are normally fitted with an experimental or close-to-experimental accuracy using a "semirigid" model based on a polynomial effective Hamiltonian.

It should be noted that rovibrational patterns of different polyads overlap for high J values even for low-lying polyads. These overlapping can result in resonance perturbations which are not accounted for by the relations (1a) and (1b). One of such examples is the resonance interaction of rotational levels of the vibrational states (110) and (101) belonging to the second dyad and to the first triad. Such interactions are, as a rule, localized and perturb few series of levels. For example, the interaction occurs between the two pair of levels $J_{K_a K_c} = 41_{14 27}$, $42_{14 29}$ of the state (101) and $41_{17 25}$, $42_{17 25}$ of the state (110),* unperturbed levels being separated by + 0.095 and - 0.226 cm⁻¹, respectively.

To describe the overlapping of RV levels between different polyads, two approaches are used. The first one is applied if the interaction is very localized and involves a small number of levels, as in the above example or in the case of interaction of the states (201) and (130) (Ref. 9). In this case polyads are usually treated in a separate way, and pairs of perturbed levels together with the type of interaction which causes these perturbations are just pointed out. Otherwise, if a large number of levels are involved in an inter-polyad resonance, one have to construct an extended polyad including all interacting states. In a latter case a single interaction parameter does not usually suffice to describe a resonance.^{11–13}

* A. Barbe, S. Mikhailenko, and V.I.G. Tyuterev, Private Communication.

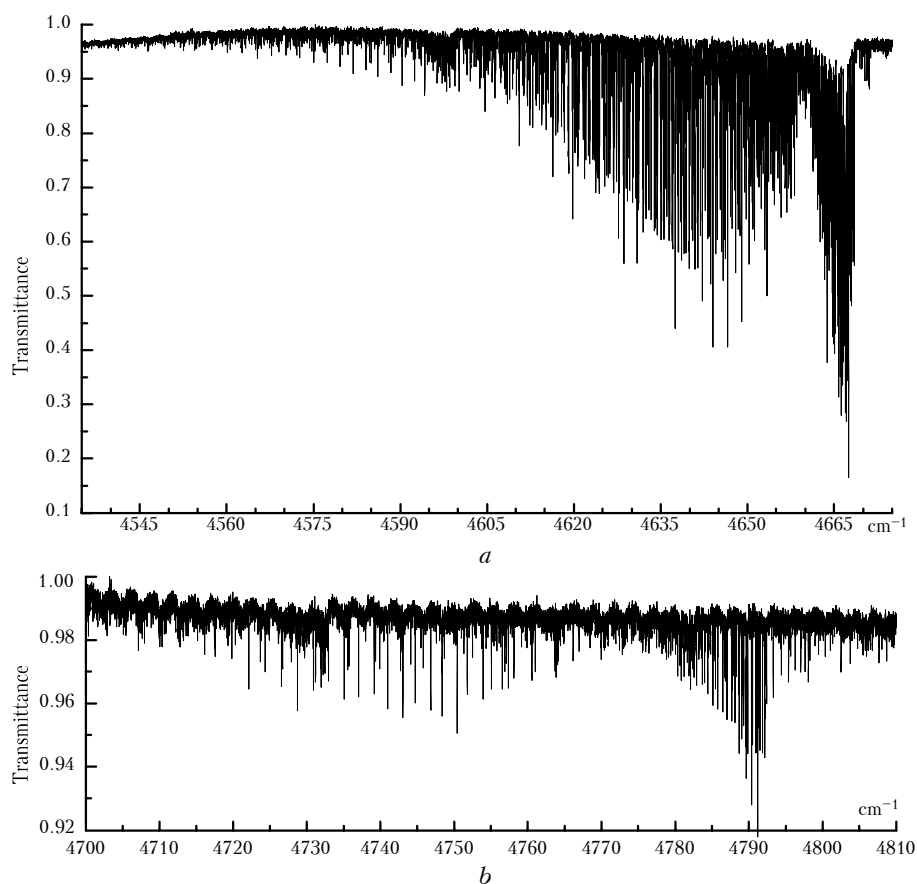


Fig 3. Typical A-type band: the $\nu_1 + \nu_2 + 3\nu_3$ band in the region of 4640 cm^{-1} . $P_{\text{O}_3} = 37.55 \text{ Torr}$, $L = 3616 \text{ cm}$ (a); typical B-type band: the $2\nu_1 + \nu_2 + 2\nu_3$ band in the region of 4750 cm^{-1} . $P_{\text{O}_3} = 38.58 \text{ Torr}$, $L = 3616 \text{ cm}$ (b).

Spectrum in the region below 3000 cm^{-1}

The results of research into ozone rovibrational spectra in the region from microwave to mid-infrared are currently presented in various atlases and databases of spectroscopic information. Most intense bands in the above-indicated region are the following: ν_3 (band center $\nu_0 = 9.6 \mu\text{m}$, integrated intensity $S_V = 1.41 \cdot 10^{-17}$), $\nu_1 + \nu_3$ ($\nu_0 = 4.74 \mu\text{m}$, $S_V = 1.24 \cdot 10^{-18}$), ν_2 ($\nu_0 = 14.27 \mu\text{m}$, $S_V = 5.92 \cdot 10^{-19}$), ν_1 ($\nu_0 = 9.07 \mu\text{m}$, $S_V = 5.40 \cdot 10^{-19}$), and $\nu_2 + \nu_3 - \nu_2$ ($\nu_0 = 9.75 \mu\text{m}$, $S_V = 4.64 \cdot 10^{-19}$). The integrated intensity S_V is given in $\text{cm}^{-1}/(\text{mol} \cdot \text{cm}^{-2})$ at $T = 296 \text{ K}$.

The recent atlas of ozone spectra, Ref. 19, provides the information on 77 bands of the three isotopic species of the ozone molecule $^{16}\text{N}_3$, $^{16}\text{N}^{16}\text{N}^{18}\text{N}$, and $^{16}\text{N}^{18}\text{N}^{16}\text{N}$ in the $0\text{--}3400 \text{ cm}^{-1}$ region. This atlas mainly lists high-accuracy calculated data on the positions and intensities of rotational and rovibrational lines. Updated and more complete versions of the atlas¹⁹ are included in the databases GEISA-97 (Ref. 20) and HITRAN-98 (Ref. 21). The GEISA-97 database includes about 282000 lines of IR transitions for five isotopic species of the ozone molecule. The HITRAN-98 database contains the information on 145106 rovibrational lines of the main isotopic specie of ozone in the region from 0 to 3000 cm^{-1} . The data of the

GEISA-97 database for the main isotopic specie are more complete than the data included in HITRAN-98. The data on four other isotopic species ($^{16}\text{N}^{16}\text{N}^{18}\text{N}$, $^{16}\text{N}^{18}\text{N}^{16}\text{N}$, $^{16}\text{N}^{16}\text{N}^{17}\text{N}$ and $^{16}\text{N}^{17}\text{N}^{16}\text{N}$) in the both databases coincide and cover the region from 0.2 to 1178 cm^{-1} .

Below we describe more recent studies which provide more detailed information on the bands belonging to this region. This information has not been yet included in the currently existing atlases and databases.¹⁹⁻²¹ Practically all laboratory spectra discussed below were recorded with the Fourier transform spectrometer of the *Groupe de Spectrométrie Moléculaire at Atmosphérique de l'Université Reims Champagne-Ardenne (France)*. The description of this spectrometer, as well as the procedure of spectra recording and line parameters measurements can be found in Ref. 22. The spectra recorded with this spectrometer allow to obtain highly accurate information. The relative accuracy of determination of line centers is $1 \cdot 10^{-4} \text{ cm}^{-1}$, while the absolute accuracy is $(4\text{--}5) \cdot 10^{-4} \text{ cm}^{-1}$. Errors in determination of intensities of good isolated lines do not normally exceed 5-7%. For very weak lines, if absorption at the line center is 1-2%, the error in intensity can be 15-20%, what is an acceptable result for such lines.

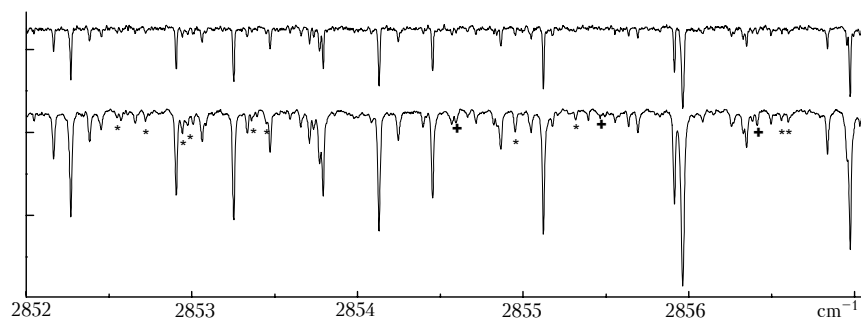


Fig. 4. Experimental spectrum of the $2\nu_1 + \nu_2$ band in the region of 2855 cm^{-1} at two different values of the ozone pressure.

Figure 4 presents, as an example, the spectrum of the $2\nu_1 + \nu_2$ band near 2855 cm^{-1} . The spectra were recorded at room temperature, with the optical path length of 3212 cm , and the ozone pressure of 11.9 Torr (upper spectrum) and 20.7 Torr (lower spectrum). The spectra are vertically shifted relative to each other for better visualization. The symbol (+) on the lower panel marks the lines of the $\nu_1 + \nu_2 + \nu_3$ band; the symbol (*) marks the lines of the hot $\nu_1 + 3\nu_3 - \nu_2$ band. Note that the marked lines have the intensity of $(3-5) \times 10^{-26}\text{ cm}^{-1}/(\text{mol}\cdot\text{cm}^{-2})$ at $T = 296\text{ K}$. The signal-to-noise ratio for these spectra was 800.

The region of $7\text{ }\mu\text{m}$ was studied in Ref. 7 using on the satellite data. This paper presents the parameters of two bands: $2\nu_2$ and $\nu_1 + \nu_3 - \nu_2$. Parameters of the transitions were determined from 27 lines of the $2\nu_2$ band and 32 lines of the $\nu_1 + \nu_3 - \nu_2$ band. More recent papers^{23,24} present the results of the analysis of laboratory spectra in the same spectral region. The spectrum was recorded with the resolution of 0.007 cm^{-1} , at the ozone pressure $p_{\text{O}_3} = 32.4\text{ Torr}$, the path length of 3212 cm , and the signal-to-noise ratio $S/N \approx 500$. It has been shown that the region under study includes, in addition to bands studied in Ref. 7, the lines of two other bands: $3\nu_2 - \nu_2$ and $2\nu_3 - \nu_2$. The analysis of the laboratory spectrum has allowed to refine information on two earlier studied bands and to obtain new information on two other bands. The integrated intensities of the bands in this region are the following: $S_V(\nu_1 + \nu_3 - \nu_2) = 9.665 \cdot 10^{-22}$, $S_V(2\nu_2) = 5.328 \cdot 10^{-22}$, $S_V(3\nu_2 - \nu_2) = 2.906 \cdot 10^{-22}$, and $S_V(2\nu_3 - \nu_2) = 1.095 \cdot 10^{-22}$ in $\text{cm}^{-1}/(\text{mol}\cdot\text{cm}^{-2})$ at $T = 296\text{ K}$.

In the region of the $\nu_1 + \nu_3$ band there is the very weak $3\nu_2$ band. This band can hardly be recorded because most of its lines are too weak as compared to the lines of $\nu_1 + \nu_3$ band. Only few lines were actually observed,¹ which "borrow" their intensity from the strong $\nu_1 + \nu_3$ band due to resonance mixing of upper-state wave-functions. Rovibrational levels of (030) state obtained from these perturbations are in a good agreement with extrapolations bases on the $3\nu_2 - \nu_2$ band analysis. The presence of this interaction leads to marked anomalies in the positions of the lines of the $\nu_1 + \nu_3$ band⁶ and to the decrease in the intensity of these lines. Note that the intensities of the observed lines of the $3\nu_2$ band are well described by mixing of

the states (030) and (101) on the assumption that the parameters of the transition moment of this band are negligibly small.

Ref. 25 present the results of new analysis of the ozone spectrum in the $2600-2900\text{ cm}^{-1}$ region. Ozone absorption in this region is mainly due to the three bands: $\nu_1 + \nu_2 + \nu_3$, $\nu_2 + 2\nu_3$, and $2\nu_1 + \nu_2$. The set of experimental data for line positions and intensities is significantly larger as compared to the data set Ref. 8, the accuracy of their fit was also improved. The root mean square (RMS) deviation for line position calculations was $5.6 \cdot 10^{-4}\text{ cm}^{-1}$, and the RMS relative deviation for intensities of 780 lines of the three bands included in the fit was 5.5%. The complete spectrum of these bands is calculated up to J and K_a equal to 70 and 23, respectively. Based on the parameters obtained for the states (012), (111), and (210), the hot bands in the $1860-2300\text{ cm}^{-1}$ region are calculated. Besides the refinement of the characteristics of the bands under study, the Ref. 25 reports a more realistic estimates (as compared to previous ones) of the vibrational energy and rotational constants of the (040) state. This "dark-state" analysis was possible due to the resonance interaction between the rotational levels of the state (040) and those of the states (111) and (012).

Vibrational states ($\nu_1 \nu_2 \nu_3$) with $\nu_2 = 3$

Until recently the rotational structure of no any vibrational state ($\nu_1 \nu_2 \nu_3$) with $\nu_2 = 3$ was experimentally available, because all the corresponding bands in the IR region are very weak and fall in the regions of stronger bands. The detailed analysis of weak bands in various spectral ranges allowed to obtain a significant information on RV levels of the following states: (030), (130), (031), and (131).

The (131) state turned out to be the first studied state of this type; the corresponding vibrational term value is $e_V(131) = 4122.069\text{ cm}^{-1}$ (Ref. 26). Two bands formed by transitions to this state: the hot $\nu_1 + 3\nu_2 + \nu_3 - \nu_2$ band in the region of 3400 cm^{-1} and the cold $\nu_1 + 3\nu_2 + \nu_3$ band in the region of 4100 cm^{-1} , were studied. Experimental positions of rovibrational spectral lines were used to determine more than 160 energy levels with the maximum values of the rotational

quantum numbers $J = 33$ and $K_a = 9$. The whole set of energy levels is described within the framework of the isolated state model with the RMS deviation of 0.002 cm^{-1} , the maximum discrepancy between the experimental and calculated energy levels being 0.006 cm^{-1} . The analysis of intensities of rovibrational lines allowed determination of the parameters of transition moments of the bands under study and calculation of their integrated intensities. The hot band has the integrated intensity $S_V(v_1 + 3v_2 + v_3 - v_2) = 7.06 \cdot 10^{-23}$ and lies in the region of the stronger bands $v_1 + 2v_2 + v_3$ and $2v_2 + 2v_3$ with the integrated intensities $S_V = 74.4 \cdot 10^{-23}$ and $S_V = 15.8 \cdot 10^{-23}$, respectively.²⁷ For the cold band, the parameter of the transition moment was estimated; this band turned out to be three times weaker than the hot band, $S_V(v_1 + 3v_2 + v_3) = 2.23 \cdot 10^{-23}$ (Ref. 26), and also to lie in the region of the stronger band $2v_1 + 2v_3$ with the intensity $S_V = 11.8 \cdot 10^{-23}$ (Ref. 28). All above intensities S_V are given in $\text{cm}^{-1}/(\text{mol} \cdot \text{cm}^{-2})$ at $T = 296 \text{ K}$.

As was noted above, Ref. 23 presents the results of the analysis of the $3v_2 - v_2$ band in the $7 \mu\text{m}$ region. The spectral line positions of this band were used to fit about 180 energy levels of the state (030) with the rotational quantum numbers up to $J = 39$ and $K_a = 9$. It should be noted that because of weakness and high density of spectral lines in this region, the accuracy of determination of the upper energy levels does not exceed $(1-2) \cdot 10^{-3} \text{ cm}^{-1}$ even for the strongest and relatively isolated lines. The data obtained were processed within the framework of the isolated state model. This allowed the RMS deviation of fit of $3.5 \cdot 10^{-3} \text{ cm}^{-1}$ to be achieved and the vibrational energy, rotational constants, and centrifugal distortion parameters of the (030) state to be determined. Further, more detailed, analysis of the (030) state should be conducted within the resonance model including the states (002), (101), and (200).

The states (130) and (031) were studied in Ref. 29. In the region of $2300-2600 \text{ cm}^{-1}$ we found a sufficiently large number of lines not belonging to the $v_1 + 2v_2$ and $2v_2 + v_3$ bands studied in Ref. 10. These lines were assigned to the hot $v_1 + 3v_2 - v_2$ and $3v_2 + v_3 - v_2$ bands. Note that the line intensities of the hot bands do not exceed 5–10% of the line intensities of corresponding cold bands. So, to assign the former with certainty, the high-quality spectrum is needed: signal-to-noise ratio should be at least 500 at the ozone pressure of 30 to 40 Torr and path length of 30 to 60 m. We succeeded to assign more than 500 lines in that range. The validity of the assignment was supported by finding weak lines of the $3v_2 + v_3$ band in the region $3060-3105 \text{ cm}^{-1}$ among rather intense lines of the $v_1 + 2v_3$ band. Figure 5 presents the J -, K_a -diagram showing the range of the rotational quantum numbers of energy levels of the states (130) and (031), corresponding to lines assigned in the spectrum. Such diagrams illustrate a state of knowledge of rotational structure for the vibrational states.

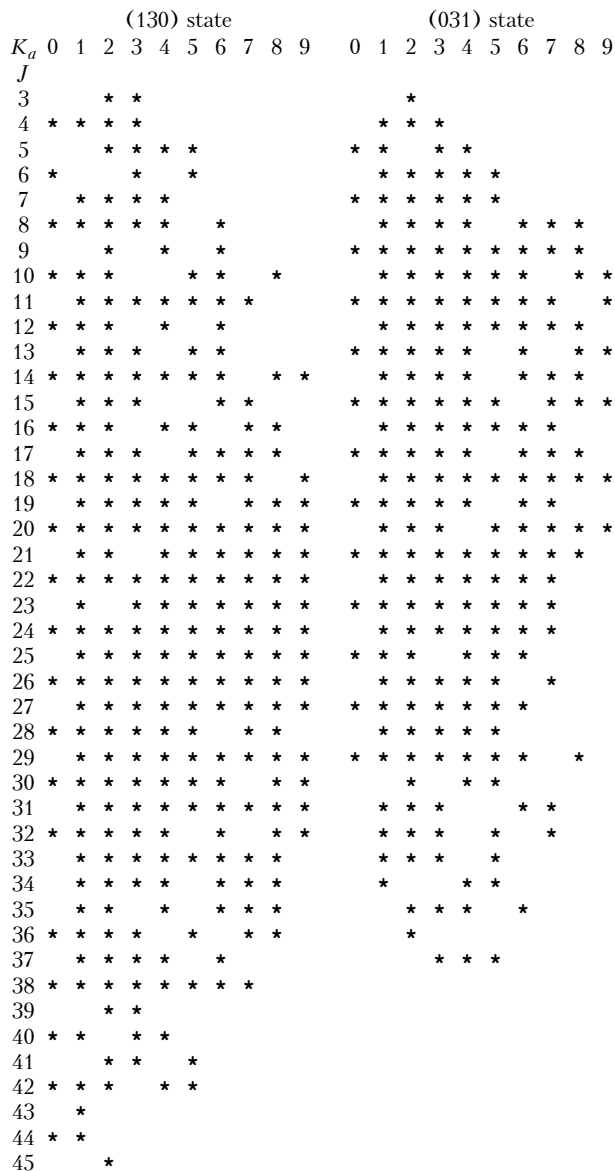


Fig. 5. J -, K_a -diagram of the rotational levels of the (130) and (031) states corresponding to experimentally recorded transitions.

480 energy levels of the states (130) and (031) up to the maximum rotational quantum numbers $J = 45$ and $K_a = 9$ were recovered with the experimental accuracy of $(0.8-1.5) \cdot 10^{-3} \text{ cm}^{-1}$. According to the polyad schemes following from relations (2) and (3), these two states should form a dyad with a resonance Coriolis coupling between them. Our calculations showed that it was however possible to fit well the obtained set of experimental data (with $\text{RMS} = 1.2 \cdot 10^{-3} \text{ cm}^{-1}$) using a simple isolated state model. This can be explained by the fact that for the energy levels observed under the experimental conditions²⁹ the mixing coefficients do not exceed 1%, whereas the maximum mixing ($\sim 35\%$) of wave functions of these states appears for quantum numbers $K_a = 17, 18$ and $J = 35-40$ which correspond to transitions below the observable intensity threshold.

Table 1. Ozone RV bands absent in the databases¹⁹⁻²¹ in the region 2300–3600 cm⁻¹

Band	Spectral region, cm ⁻¹	Intensity S_V (10 ⁻²³ cm ⁻¹ /(mol · cm ⁻²) at $T = 296$ K)*	Number of lines	Ref.
$3\nu_2 + \nu_3 - \nu_2$	2335–2410	1.6	606	29
$\nu_1 + 3\nu_2 - \nu_2$	2435–2540	0.5	315	29
$3\nu_2 + \nu_3$	3020–3120	4.5	931	29
$\nu_1 + 3\nu_2 + \nu_3 - \nu_2$	3360–3442	7.06	1167	26
$\nu_1 + 2\nu_2 + \nu_3$	3375–3480	74.4	1926	27
$2\nu_2 + 2\nu_3$	3245–3510	15.8	2502	27

* The sum of line intensities exceeds 10⁻²⁶ cm⁻¹/(mol·cm⁻²) at $T = 296$ K.

The observed intensities of the $\nu_1 + 3\nu_2 - \nu_2$ and $3\nu_2 + \nu_3 - \nu_2$ bands are well described with the account of the parameters of transition moments of the bands $\nu_1 + 2\nu_2$ and $2\nu_2 + \nu_3$ only (Ref. 10). The lines of the $3\nu_2 + \nu_3$ band in the region 3060–3105 cm⁻¹ were used to estimate the parameter μ_1 corresponding to the first term of expansion of the effective transition moment for this band $\mu_1^{(3\nu_2+\nu_3)} = 2 \cdot 10^{-4} D$. The attempts to find lines of the $\nu_1 + 3\nu_2$ band failed. According to our estimates, the upper limit for the strongest lines of this band does not exceed 3 · 10⁻²⁶ cm⁻¹/(mol·cm⁻²) at $T = 296$ K.

The results of studies of the rotational structure of the (030), (031), (130), and (131) states indicate that most of presently available $\nu_2 = 3$ data can be well described within the approximation of isolated vibrational states. This is explained, first, by weakness of the bands corresponding to transitions to these states and, consequently, low accuracy of experimental data. The second cause is that high-excited rotational states which should be in resonance correspond to very weak lines currently not observed in experiments. The exception is the series of eight levels of the (030) state and four levels of the (130) state. These two cases serve as instructive examples of the high-order Coriolis resonance due to the relation (1b). To adequately describe these levels, one should take into account the interaction with the states (101) and (201), respectively.

The integral characteristics of some bands described in this section are given in Table 1 whose fourth column shows the number of lines with intensities higher than 1 · 10⁻²⁶ cm⁻¹/(mol·cm⁻²) at $T = 296$ K.

No experimental information is currently available on the rotational structure of vibrational state ($\nu_1\nu_2\nu_3$) with $\nu_2 > 3$. The integrated intensities of both hot and cold bands corresponding to these states are smaller than 1 · 10⁻²³ cm⁻¹/(mol·cm⁻²), the intensities of individual lines likely do not exceed (1–2) · 10⁻²⁶ cm⁻¹/(mol·cm⁻²) at $T = 296$ K. Besides, they fall in the regions of other, stronger bands. These reasons make the vibrational states under study hardly observable even at further increase of the ozone optical depth and higher signal-to-noise ratio. The information on these states can be derived indirectly from "dark-state" analysis of their interactions with other states.

Spectrum in the region 3000–3600 cm⁻¹

The ozone absorption spectrum in the indicated region is caused by two groups of bands. The first group incorporates three-quanta bands ($\Delta\nu = 3$), that is, transitions to the tetrad of interacting states {(003), (102), (201), (300)}. These bands were studied in Refs. 9 and 30. The second group of four-quanta bands ($\Delta\nu = 4$) incorporates the transitions to the triad {(022), (121), (220)} and dyad {(031), (130)}. The above-mentioned triad was studied in Ref. 27, while the dyad was considered in the previous section. The strongest band in this region is $3\nu_3$. Besides the indicated bands, the spectrum in this region includes several more weaker hot bands corresponding to transitions from the state (010) to higher vibrational states.

The tetrad {(003), (102), (201), (300)} was a subject of several studies, however by now it is not completely described. Camy-Peyret et al.⁹ have found line positions and intensities for the three bands: $3\nu_3$, $\nu_1 + 2\nu_3$, and $2\nu_1 + \nu_3$ up to $J = 50$ and $K_a = 16$. The study of Ref. 30 supplemented these data with the information on the $3\nu_1$ band for the same range of the rotational quantum numbers. However, the maximum for intra-polyad interactions correspond to rotational quantum numbers J and K_a above indicated range. As a result, an extrapolation to higher quantum numbers gives significant errors both in line positions and in intensities. In the available laboratory spectra the lines of the indicated bands up to $J = 70$ and $K_a = 20$ are actually observed.**

Moreover, as was noted in Ref. 9, some levels of the state (201) are perturbed by the resonance with the state (130). In the range $35 < J < 50$ for $K_a = 12$ the state (102) interacts with the upper state (210) of the low-lying triad {(012), (111), (210)} (see Fig. 2b). The levels of the state (003) with $K_a = 16$ interact with the levels $K_a = 17$ of the state (210) at $J > 20$. All these interactions result in rather strong anomalies in line positions. For example, for the band $\nu_1 + 2\nu_3$ the perturbations in line positions achieve 0.1 cm⁻¹, and for the $3\nu_3$ band they may be as large as 0.5 cm⁻¹***

** S. Mikhailenko, A. Barbe, V.I.G. Tyuterev, and J.J. Plateaux, in: *XIIIth Symposium on High Resolution Molecular Spectroscopy*, Poster E4.

*** *ibid.*

The Ref. 27 reports the study of the bands $2\nu_2 + 2\nu_3$ and $\nu_1 + 2\nu_2 + \nu_3$ belonging to the triad $\{(022), (121), (220)\}$. The weakest band $2\nu_1 + 2\nu_2$ corresponding to transitions to the state (220) is not yet analyzed. Besides, the anomalies in positions of some energy levels of the (121) state due to the resonance with the (050) state are still to be described. The characteristics of the bands of this triad are included in Table 1.

The accuracy of calculation of integral intensities of the hot bands lying in this region, such as $\nu_2 + 3\nu_3 - \nu_2$, $\nu_1 + \nu_2 + 2\nu_3 - \nu_2$, and $\nu_1 + 3\nu_3 - \nu_2$, is unlikely higher than 40–50%. In our opinion, all the above-said allows the region 3000–3600 cm^{-1} to be considered as promising for new research in order to refine its overall characteristics and the rotational structure of the band periphery corresponding to transitions to high-excited rotational levels of the indicated vibrational states.

Spectrum in the region above 3600 cm^{-1}

The high-resolution absorption spectrum of ozone in the region higher than 3600 cm^{-1} is now studied up to 5800 cm^{-1} . Let us consider separately the groups of bands with the same $\Delta\nu \equiv \sum_i |\Delta\nu_i|$, because they, as a rule, lie in different, increasingly high-frequency, spectral ranges. While speaking of bands with a given $\Delta\nu$, we limit ourselves by bands falling in the above-indicated spectral region only. Note that there are combination bands with large $\Delta\nu$ which should however lie below 3600 cm^{-1} . For example, the $3\nu_3 - \nu_1$ band ($\Delta\nu = 4$) lies in the region 1895–1960 cm^{-1} , whereas the bands $4\nu_3 - \nu_1$, $3\nu_1 + \nu_2 - \nu_3$, and $\nu_1 + 3\nu_3 - \nu_2$ ($\Delta\nu = 5$) lie in the region from 2850 to 3350 cm^{-1} .

Observable bands in this region correspond to transitions to the states $(\nu_1\nu_2\nu_3)$ with $\nu_2 = 0, 1$, and 2. The only exception is the very weak $\nu_1 + 3\nu_2 + \nu_3$

band. The general view of the ozone absorption spectrum in the region from 3400 to 5800 cm^{-1} is shown in Figs. 6–8. It should be noted that the region 3500–3950 cm^{-1} includes some strong bands of q n_2 and m_2n . These molecules are always present as residual or calibration gases in the working volume of a spectrometer, therefore even high-quality laboratory spectra are complicated by their absorption lines in the indicated region, what is well seen in Fig. 6. Strong lines in Figs. 7 and 8 in the region 5100–5600 cm^{-1} belong to the $\nu_2 + \nu_3$ band of water vapor. In Fig. 7 one can also see the $12^{01} \leftarrow 00^{00}$ band of carbon dioxide in the region of 4978 cm^{-1} .

Bands with $\Delta\nu = 4$

The cold bands of this type are formed by the transitions from the ground vibrational state to the levels of the tetrad $\nu_2 = 1$ $\{(013), (112), (211), (310)\}$ and pentad $\nu_2 = 0$ $\{(004), (103), (202), (301), (400)\}$. They lie in the range from 3550 to 4300 cm^{-1} ; the stronger bands are the A-type bands. The most intense band in this region is $\nu_1 + 3\nu_3$. Table 2 gives the brief information on the bands considered below.

Table 2. Ozone RV bands with $\Delta\nu = 4$ above 3600 cm^{-1}

Band	Region, cm^{-1}	Intensity S_V ($10^{-22} \text{ cm}^{-1}/(\text{mol}\cdot\text{cm}^{-2})$) at $T = 296 \text{ K}$	Ref.
$\nu_2 + 3\nu_3$	3578–3710	55.3	32
$\nu_1 + \nu_2 + 2\nu_3$	3585–3840	8.0	32
$2\nu_1 + \nu_2 + \nu_3$	3762–3866	13.0	34
$3\nu_1 + \nu_2$	3890–4050	4.5	21
$\nu_1 + 3\nu_3$	3910–4033	137.8	21
$4\nu_3$	3890–4060	5.7	21
$2\nu_1 + 2\nu_3$	4015–4214	1.18	28
$3\nu_1 + \nu_3$	4170–4265	2.5	11

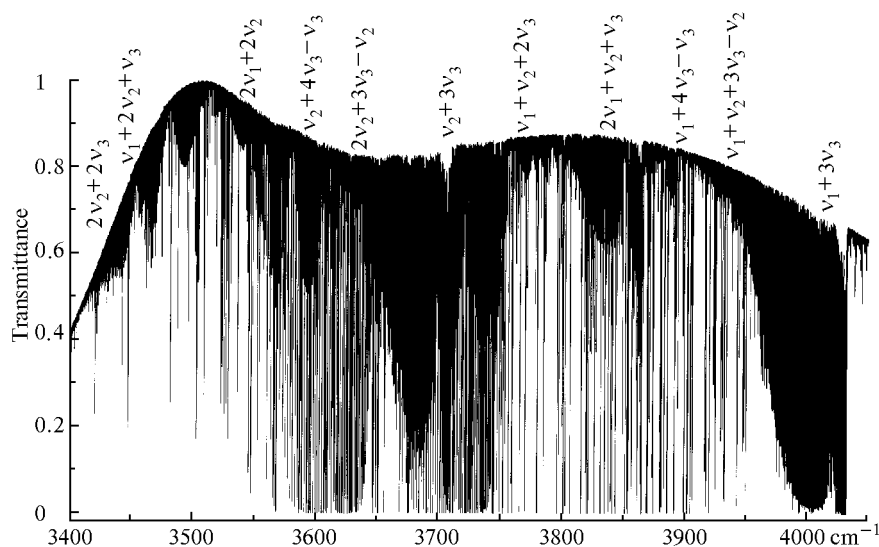


Fig. 6. General view of the ozone absorption spectrum in the region 3400–4050 cm^{-1} . $P_{\text{O}_3} = 21.8 \text{ Torr}$, $L = 3212 \text{ cm}$.

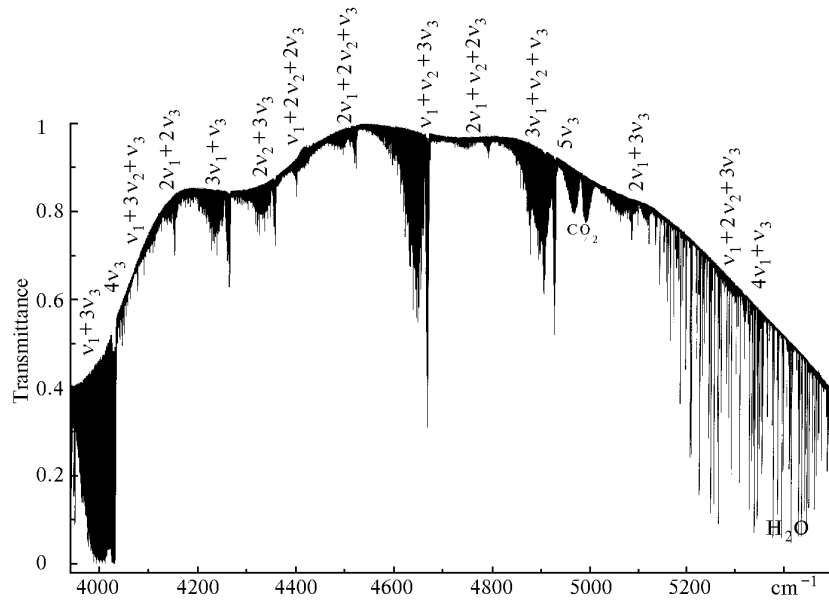


Fig. 7. General view of the ozone absorption spectrum in the region 3940–5500 cm^{-1} . $P_{\text{O}_3} = 26.0$ Torr, $L = 3212$ cm.

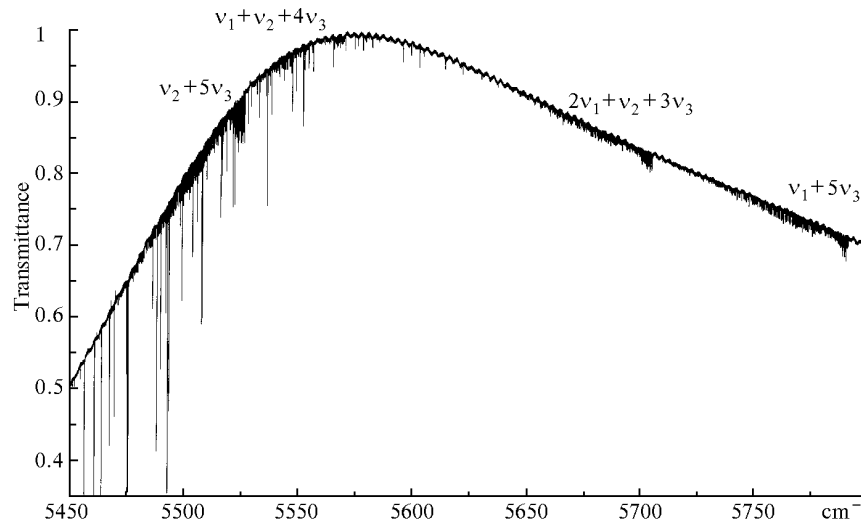


Fig. 8. General view of the ozone absorption spectrum in the region 5450–5800 cm^{-1} . $P_{\text{O}_3} = 26.9$ Torr, $L = 3212$ cm.

In the databases of spectroscopic information^{20,21} the ozone absorption in the region above 3600 cm^{-1} is presented by only five bands: $v_1 + v_2 + 2v_3$ and $v_2 + 3v_3$ below 3762 cm^{-1} and $4v_3$, $v_1 + 3v_3$, and $3v_1 + v_2$ in the region 3892–4060 cm^{-1} . The first two bands result from the research reported in Ref. 31, however only the band $v_2 + 3v_3$ was directly observed while for the $v_1 + v_2 + 2v_3$ band only estimates were given. In the more recent study, Ref. 32, both bands were analyzed. It is interesting to note that the integrated intensity $S_V(v_1 + v_2 + 2v_3)$ given in Ref. 32 largely exceeds (nearly by factor 6) the value previously reported in Ref. 31. Note that the intensities of RV lines in Ref. 32 were determined experimentally, and the parameters of the transition moment for that band were determined from the solution of the inverse problem, whereas in Ref. 31 those parameters were considered as negligible. The two bands under discussion are formed by

the transitions to the levels of the states (013) and (112). Being a part of the tetrad $v_2 = 1$ of interacting states $\{(013), (112), (211), (310)\}$, these states nevertheless are well described within the framework of the dyad model ignoring the interaction with the two upper-lying vibrational states. This is because the separations between the states (211) and (112), as well as the states (310) and (211) exceed 110 cm^{-1} . As was noted above, the database of spectroscopic information²¹ currently contains only the calculated data from Ref. 31.

The analysis of the group of bands lying in the region 3850–4100 cm^{-1} was performed in Ref. 14. More recent paper³³ gives the corrected set of spectroscopic parameters for the states (004), (103), and (310) derived from the study of the hot $4v_3 - v_3$ band in the region of 3.3 μm . In spite of satisfactory, on the whole, description of the above-indicated bands, the

extrapolation to higher rotational quantum numbers does not give good results both for line positions and for intensities. The average accuracy is 0.003 cm^{-1} for the energy levels, however the maximum discrepancy between the experimental and calculated energy levels exceeds 0.030 cm^{-1} . The $3\nu_1 + \nu_2$ band is almost 30 times weaker than the $\nu_1 + 3\nu_3$ band and lies in the same region as the $\nu_1 + 3\nu_3$ band which is the strongest band in this spectral region. Because of relatively few data available for the state (310), the interaction parameters turn out to be poorly determined, what manifests itself in poor results of extrapolation. Besides, for a correct description of all levels of the state (103), the resonance interaction of this state with the state (032) should be taken into account.

Reference 34 is devoted to determination of the parameters of the $2\nu_1 + \nu_2 + \nu_3$ band lying between the two groups of bands discussed above. The spectrum used in Ref. 34 was recorded at 49 Torr and the path length was 36 m. However, the signal-to-noise ratio was not very high ($S/N \approx 250$). That circumstance and other technical problems allowed to assign transitions which correspond to energy levels of the state (211) up to $J = 40$ and $K_a = 12$ only. It was found that some levels of that state with $K_a = 3, 4$ at $20 < J < 40$ are perturbed by the resonance interaction of the Coriolis type with the levels of the state (140). The currently available spectra with high signal-to-noise ratio $S/N \approx (500-700)$ have allowed to obtain the information on transition to the upper levels with $J \approx 55$ and $K_a \approx 20$.

The region $4015-4214 \text{ cm}^{-1}$ is occupied by the $2\nu_1 + 2\nu_3$ band.²⁸ This band presents no difficulties in assignment of spectral lines and determination of spectral parameters, except for its weakness. The experimental data are well described by the model of isolated state. This is explained by relatively large separation of the state (202) from the neighboring vibrational states of the pentad $\nu_2 = 0$ ($\approx 110 \text{ cm}^{-1}$) to which this state belongs. The accuracy of RMS deviation of the fit was $1.4 \cdot 10^{-3} \text{ cm}^{-1}$ for line positions and 15–20% for intensities. Because of the absence of perturbations, the extrapolation capabilities of the parameters obtained are rather satisfactory.

Among the studied bands with $\Delta\nu = 4$, the $3\nu_1 + \nu_3$ band has the highest frequency.¹¹ Already at the stage of assignment of this band a lot of problems arise which indicate that a correct assignment of spectral lines and a correct description of rotational energy levels of the upper vibrational state (301) require the interaction with the state (230) to be taken into account. The energy levels with small K_a values are strongly perturbed by this interaction. The band corresponding to the state (230) was not observed in the IR spectrum because it should be very weak, so the state (230) is considered currently as a "dark" state. Thus, the reliability of determination of the parameters of this state is low, what results in a poor description of the rotational energy levels of the state (301).

In conclusion it should be noted that up to date two bands belonging to the set under study are still to be investigated: $4\nu_1$ (near 4370 cm^{-1}) and $2\nu_1 + 2\nu_2$ (in the region $3500-3650 \text{ cm}^{-1}$). Lines of these bands are present in the recorded spectra, however the assignment is hampered by their weakness and possible resonance perturbations. The hot $\nu_1 + \nu_2 + 3\nu_3 - \nu_2$ band in the region of the $\nu_1 + 3\nu_3$ band is also to be noted. The line positions of this band are well-known, but accurate information on line intensities is not yet available. According to estimates, the integral intensity of this band is about 5–7% of the intensity of the $\nu_1 + 3\nu_3$ band, thus exceeding the intensity of such a band as $2\nu_1 + 2\nu_3$ (see Table 2).

Bands with $\Delta\nu = 5$

These bands lie in the region from 4300 to 5330 cm^{-1} , and their intensity is in average an order of magnitude lower than the intensity of the bands with $\Delta\nu = 4$. Nine of thirteen bands investigated up to now are the bands of type A. Table 3 gives their integral characteristics.

The $2\nu_2 + 3\nu_3$ band corresponding to the upper vibrational state (023) lies in the region of 4340 cm^{-1} (Ref. 15). The (023) state along with the states (122) and (400) form the triad of interacting states. The latter two states were included in the processing of line positions and intensities of the $2\nu_2 + 3\nu_3$ band, but only as dark states. As a result, the data obtained in Ref. 15 were described accurate to $1.9 \cdot 10^{-3} \text{ cm}^{-1}$ for line positions and 15% for intensities. The more recent spectra have allowed assigning the band $\nu_1 + 2\nu_2 + 2\nu_3$ and to obtain more accurate information on the $2\nu_2 + 3\nu_3$ band. The results of the analysis and processing of these data will be reported later. The region of the p -branch of the $2\nu_2 + 3\nu_3$ band in the region $4315-4332 \text{ cm}^{-1}$ is shown in Fig. 9 to illustrate the quality of the recorded spectrum and typical absorption in line centers. The sufficiently strong line at 4323.06 cm^{-1} corresponds to the superposition of two lines with $K_a = 0$ and 1 for $J = 19$.

Table 3. RV bands of ozone above 4050 cm^{-1} with $\Delta\nu=5$

Band	Region, cm^{-1}	Intensity S_V ($10^{-22} \text{ cm}^{-1}/(\text{mol}\cdot\text{cm}^{-2})$) at $T = 296 \text{ K}$)	Ref.
$\nu_1 + 3\nu_2 + \nu_3$	4055–4150	0.2	26
$2\nu_2 + 3\nu_3$	4280–4358	2.4	15
$2\nu_1 + 2\nu_2 + \nu_3$	4440–4526	1.1	35
$\nu_1 + 2\nu_2 + 3\nu_3 - \nu_2$	4520–4600	0.68	36
$\nu_2 + 4\nu_3$	4520–4700	1.7	17
$3\nu_1 + 2\nu_2$	4540–4700	0.5	17
$\nu_1 + \nu_2 + 3\nu_3$	4555–4670	8.8	17
$2\nu_1 + \nu_2 + 2\nu_3$	4700–4850	0.5	12
$3\nu_1 + \nu_2 + \nu_3$	4820–4960	3.66	16
$5\nu_3$	4840–4930	5.45	16
$\nu_1 + 4\nu_3$	4820–4960	0.97	16
$2\nu_1 + 3\nu_3$	5000–5086	1.33	13
$4\nu_1 + \nu_3$	5250–5320	0.85	36

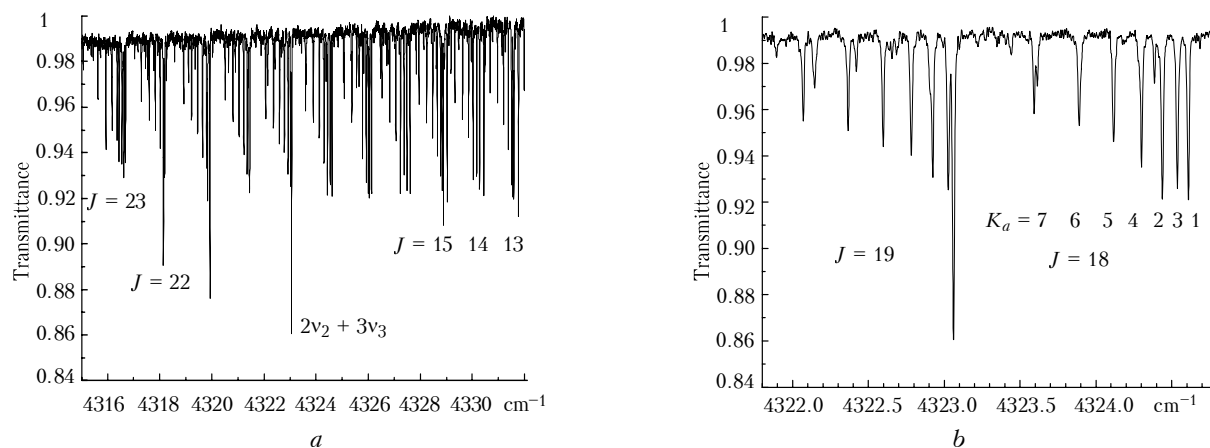


Fig. 9. A part of the spectrum of the $2\nu_2 + 3\nu_3$ band in the region $4315\text{--}4332\text{ cm}^{-1}$, $P_{\text{O}_3} = 26.0\text{ Torr}$, $L = 3212\text{ cm}$ (a); and in the region 4323.5 cm^{-1} , $P_{\text{O}_3} = 26.0\text{ Torr}$, $L = 3212\text{ cm}$ (b).

The $2\nu_1 + 2\nu_2 + \nu_3$ band lying in the region around 4500 cm^{-1} is formed by the transitions to the vibrational state (221) belonging to the same polyad (tetrad $\nu_2 = 2$) as the states (023) and (122). As the above-considered state (202), the state (221) is well described as an isolated state.³⁵ The strongest lines achieve 4% in absorption at the ozone pressure of 38 Torr and the path length of 36 m. As a result, the accuracy in determination of the line positions does not exceed 0.001 cm^{-1} , and the error in determination of intensities is about 20%.

The transitions to the three strongly interacting states (014), (320), and (113) form absorption in the region $4530\text{--}4700\text{ cm}^{-1}$ (Ref. 17). The general view of the spectrum in this region is shown in Fig. 3a. This group of states is similar to the triad $\{(004), (310), (103)\}$ from Ref. 14. The difference is that the separation between the levels in the case is much smaller ($\approx 10\text{--}15\text{ cm}^{-1}$), therefore the interaction between the states is much stronger. Besides, the bands corresponding to these states are weaker by an order of magnitude (see Tables 2 and 3). These two circumstances make the analysis and description of this group of bands a very complicated problem. The strongest band in this region is the $\nu_1 + \nu_2 + 3\nu_3$ band. Two other bands ($\nu_2 + 4\nu_3$ and $3\nu_1 + 2\nu_2$) are weaker by almost an order of magnitude. So, it is natural that much more energy levels are determined for the state (113) than for other two states. The most of energy levels of the state (014) is determined from analysis of the hot $\nu_2 + 4\nu_3 - \nu_3$ band in the region $3550\text{--}3605\text{ cm}^{-1}$. As to the $3\nu_1 + 2\nu_2$ band, only the lines corresponding to upper levels of the state (320), which are in strong resonance with the state (113), appear in the spectrum. The accuracy of calculations for energy levels of this group of states (RMS = 0.0031 cm^{-1} , maximum discrepancy between the calculated and measured values of 0.030 cm^{-1}) does not yet achieve as the experimental accuracy. In our opinion, the explanation is a lack of information on the (320) state, what results in strong correlation between the parameters of the Hamiltonian and their poor

determinability. Figure 10 demonstrates the quality of description of the spectrum in this region. The difference between the experimental and calculated spectra does not exceed 6%, to say, it is within the error of determination of the intensities.

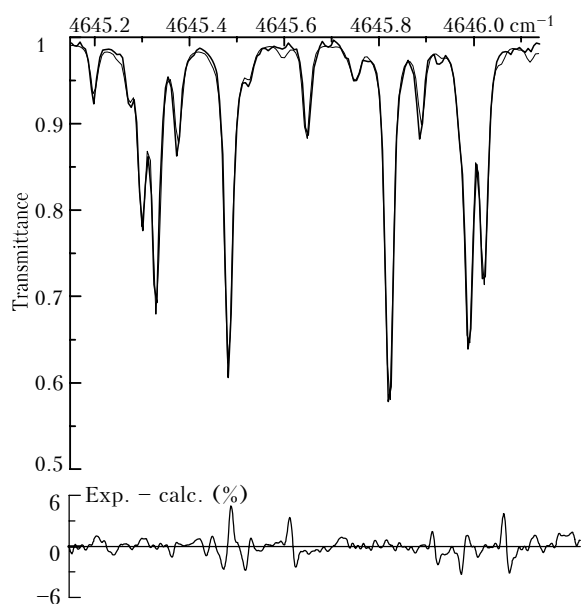


Fig. 10. Experimental and simulated spectra in the region around 4645.6 cm^{-1} . $P_{\text{O}_3} = 37.55\text{ Torr}$, $L = 3616\text{ cm}$.

The hot $\nu_1 + 2\nu_2 + 3\nu_3 - \nu_2$ band lies in the region $4519\text{--}4600\text{ cm}^{-1}$ (Ref. 36). It is formed by the transitions between the state (010) and (123). In the next section the (123) state is considered in greater detail. Here we only note that the lines of this band strongly complicate the assignment of transitions to the state (113) with the large values of J .

Reference 12 describes the $2\nu_1 + \nu_2 + 2\nu_3$ band occupying the region $4700\text{--}4855\text{ cm}^{-1}$. The line intensities of this band are below $4 \cdot 10^{-25}\text{ cm}^{-1}/(\text{mol}\cdot\text{cm}^{-2})$ at $T = 296\text{ K}$. The signal-to-noise ratio in this spectral region is about 200, therefore the line intensities are

determined with the accuracy about 20%. The analysis of anomalies in line positions demonstrates a necessity to take into account the interaction between the states (212) and (141). In this case it becomes possible to estimate the vibrational term value of the (141) state: $E^{(141)} = 4783.2 \text{ cm}^{-1}$ accurate to 0.5 cm^{-1} .

The region $4820\text{--}4960 \text{ cm}^{-1}$ is occupied by the $5\nu_3$, $3\nu_1 + \nu_2 + \nu_3$, and $\nu_1 + 4\nu_3$ bands.¹⁶ The upper vibrational states of these bands are (005), (311), and (104). They form the group of very closely lying states: unperturbed vibrational term values for the states (005) and (311) are separated by 1 cm^{-1} only. They form the triad similar to the groups of states considered in Refs. 14 and 37. Because the $\nu_1 + 4\nu_3$ band is very weak, we used the hot $\nu_1 + 4\nu_3 - \nu_3$ band lying in the $2.5 \mu\text{m}$ region to obtain the information about the (104) state. The integrated intensity of this band makes up about 3–5% of the intensity of the $\nu_1 + 3\nu_3$ band. About 780 energy levels of those three states were described accurate, on the average, to 0.0043 cm^{-1} . For 3.5% of levels the deviations were from 0.010 to 0.030 cm^{-1} . Keeping in mind the high degree of mixing of the wavefunctions of the corresponding rotational–vibrational states, this result can be considered as satisfactory. The line intensities were described accurate to 15–30%.

The analysis of the $2\nu_1 + 3\nu_3$ band in the region $5000\text{--}5086 \text{ cm}^{-1}$ (Ref. 13) is interesting, because very strong Coriolis interaction between the (203) and (132) states allows detection of the lines belonging to the $\nu_1 + 3\nu_2 + 2\nu_3$ band in the spectrum. Thus, ten energy levels of the (132) state with $K_a = 4$ and 5 for $18 < J < 32$ were determined. A RMS deviation of the fit of 492 energy levels of this dyad was of 0.0018 cm^{-1} , what is close to the experimental accuracy of determination of energy levels. The analysis performed in Ref. 13 makes it possible to estimate the vibrational term value $E^{(132)} = (5038.5 \pm 0.3) \text{ cm}^{-1}$ and to determine the rotational constants of the (132) state.

The $4\nu_1 + \nu_3$ band also belongs to the class of the bands under study ($\Delta\nu = 5$) lying near 5300 cm^{-1} (Ref. 36). Figure 11 shows the scheme of the four vibrational states in this region. Taking into account relations (1a) and (1b), it seems natural to assume that they would form two pairs of interacting states. According to the classical scheme of resonances in the ozone molecule,¹⁹ the (024) and (123) states should be perturbed by the first-order Coriolis resonance. For the pairs of states $((0\nu_2\nu_3)$ and $(1 \nu_2 \nu_3 - 1))$ at $E_{\text{VIB}} < 5000 \text{ cm}^{-1}$ this resonance is very strong, and it was observed for all the earlier studied states. For the states (401) and (330), in view of relation (1b), one would expect the manifestation of the fourth-order Coriolis resonance, as it was observed for the pairs of states (101)/(030) (Ref. 6) and (201)/(130) (Ref. 9), and (301)/(230) (Ref. 11). However, the analysis of the spectrum in this region shows that the four above mentioned states should be considered as the interacting pairs with another scheme of coupling: (123)/(330)

and (401)/(024). This means that the scheme of formation of polyads should be radically revised for high vibrational excitations.

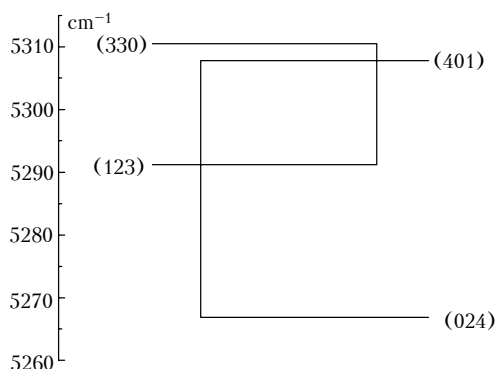


Fig. 11. The scheme of vibrational states of the ozone molecule in the region of 5300 cm^{-1} , corresponding to the observed high-order resonances.

Bands with $\Delta\nu = 6$

Such bands are much weaker, so up to date only five bands of this type have been studied, four of them are A-type bands and one is the B-type band. Because of their weakness, the corresponding upper rovibrational levels are known not as good as those for the low-lying states. The integrated intensities of these bands and their spectral regions are given in Table 4. The uncertainty of determination of the integrated intensities is within 30–35%.

Table 4. Ozone RV bands with $\Delta\nu = 6$ above 5200 cm^{-1}

Band	Region, cm^{-1}	Intensity S_V ($10^{-23} \text{ cm}^{-1}/(\text{mol}\cdot\text{cm}^{-2})$ at $T = 296 \text{ K}$)	Ref.
$\nu_1 + 2\nu_2 + 3\nu_3$	5240–5300	6.30	36
$\nu_2 + 5\nu_3$	5465–5527	9.33	37
$\nu_1 + \nu_2 + 4\nu_3$	5450–5570	1.44	37
$2\nu_1 + \nu_2 + 3\nu_3$	5640–5705	3.12	38
$\nu_1 + 5\nu_3$	5715–5792	4.58	39

The $\nu_1 + 2\nu_2 + 3\nu_3$ band lying in the same region as the $4\nu_1 + \nu_3$ band³⁶ has almost the same intensity. It is interesting to note that the hot $\nu_1 + 2\nu_2 + 3\nu_3 - \nu_2$ band lying near 4600 cm^{-1} and corresponding to the same upper vibrational state (123) has somewhat higher integral intensity than the corresponding cold band. As was mentioned above, the (123) state interacts with the upper-lying (330) state. The accuracy of calculation of the rovibrational energy levels up to $J = 35$ and $K_a = 12$ is about 0.002 cm^{-1} . The attempts to improve this description by the way of phenomenological allowance for the interactions with the neighboring states (024) and (401) were not successful. The processing of line intensities with the use of a single parameter of the effective operator of transition moment gives the accuracy about 30%.

In Ref. 37 the spectral region $5500\text{--}5570 \text{ cm}^{-1}$ was analyzed which contains two bands $\nu_2 + 5\nu_3$ (type A)

and $\nu_1 + \nu_2 + 4\nu_3$ (type B). The corresponding upper vibrational states (015) and (114) are in the resonance interactions with the states (321) and (080). The state (321) perturbs the energy levels of the (015) state for the small values of the rotational quantum number K_a , whereas the state (080) perturbs the levels for $K_a = 8, 9, \text{ and } 10$. A total of 285 rotational energy levels are fitted with the accuracy of 0.0024 cm^{-1} , what can be considered as a good result for so weak bands.

Line positions and intensities of the $2\nu_1 + \nu_2 + 3\nu_3$ band are studied in Ref. 38. To describe this band with acceptable accuracy (RMS = 0.0025 cm^{-1}), the Coriolis interaction between the states (213) and (420) was necessary to be taken into account. As a result of processing of the line positions of the studied band, the parameters of the (420) state and the mixing coefficients of the rotational energy levels of the two states were determined. In this way, it was possible to find³⁸ several lines of the $4\nu_1 + 2\nu_2$ band. This example indicates that the procedure of indirect determination of the parameters of a dark state from the observed perturbations of its interacting partner can in some cases give acceptable values possessing some predicting capabilities.

The most high-frequency rotational-vibrational band of the ozone studied so far via high-resolution IR spectroscopy is the $\nu_1 + 5\nu_3$ band.³⁹ To describe all the anomalies in this band, Chichery et al.³⁹ had to take into account the interaction of the state (105) with the states (006) and (312). The energy levels with $J < 40$ and $K_a < 13$ are reconstructed accurate to 0.002 cm^{-1} , and the intensities are reconstructed with the accuracy about 40%.

The spectra of the bands considered in this section were recorded with the resolution of 0.008 cm^{-1} at the Fourier spectrometer of the Reims University. The ozone optical density corresponded to the ozone pressure of 28.3 Torr at the path length of 3212 cm. The signal-to-noise ratio in different spectral regions varied from 200 to 350. The integrated intensities of all studied bands did not exceed $1 \cdot 10^{-22} \text{ cm}^{-1} / (\text{mol} \cdot \text{cm}^{-2})$ at $T = 296 \text{ K}$ (see Table 4).

Conclusion

This paper presents the state of the art in the research on high-resolution IR spectra of the main isotopic species of ozone molecule in various spectral regions.

The studies in the region up to 3000 cm^{-1} have the longest history. However, even in this spectral region the intensities of only relatively small number of lines of some bands are determined with the accuracy as good as 2–6% (Refs. 40–42). For most bands in this region the typical uncertainty of intensity determination is about 8–10%. The estimation is valid for the fundamental bands, whereas for the weak bands and lines corresponding to transitions to high-excited rotational states errors in determination of intensities may achieve 15–20%. The accuracy of determination of line positions

is very high; for isolated lines in the range 15–60% in absorption it is $(1-4) \cdot 10^{-4} \text{ cm}^{-1}$.

The situation changes considerably in the higher spectral region. For example, to determine with high accuracy the intensities of the $3\nu_3$ and $\nu_1 + 3\nu_3$ bands which are the strongest bands in the regions around 3000 and 4000 cm^{-1} , respectively, one has to take into account very large number of hot bands (see, for example, Ref. 33) corresponding to higher vibrational states. These bands are formed by transitions from the states (010), (100), and (001); their integrated intensities make up 3–7% of the intensity of the fundamental bands in these regions. Thus, it seems natural to estimate the accuracy in determination of intensities in the region $3000-4200 \text{ cm}^{-1}$ as 10–15%. Line positions are determined accurate to $(5-10) \cdot 10^{-4} \text{ cm}^{-1}$.

The region $4200-5000 \text{ cm}^{-1}$ is occupied by sufficiently weak bands with $\Delta v = 4$ and 5. The intensities of these bands can hardly be determined better than to 15–20%; the accuracy in determination of line positions remains sufficiently high, about 0.001 cm^{-1} . In the region $5000-5800 \text{ cm}^{-1}$, with the same accuracy of determination of line positions, the intensities are determined with an accuracy no better than 25–30%.

To study the ozone spectra above 4000 cm^{-1} , the large ozone optical depth is needed. In these studies the ozone pressure varied from 25 to 40 Torr with a path length of 32 or 36 m. Recording spectra by the methods of high-resolution Fourier spectroscopy above 6000 cm^{-1} would require an ozone optical depth increased by an order of magnitude. All the above-said makes the study of spectra in this region very complicated and rather expensive problem. To study the ozone vibrational states near the dissociation limit ($6000-9000 \text{ cm}^{-1}$), some other methods should likely be applied. It should be noted that the vibrational states in this region are very close to each other, but the bands corresponding to most states have very low intensity.

The recent analysis of weak absorption bands and high-excited rotational-vibrational states of the ozone molecule^{11,13-17,36-39} has demonstrated the necessity to take into account new resonance interactions which do not obviously follow from the standard analysis of the normal modes of a molecule. The existence of these localized resonances is due to overlapping of classical stretching polyads (with the fixed sum $\nu_{\text{str}} = \nu_1 + \nu_3$) following from the relation (1a), as the energy increases. The list of accidental resonances of high orders among high-excited vibrational states of the ozone molecule having studied by now is presented below.

- (400) $\leftarrow C \rightarrow$ (023) $\delta v = 9$ Ref. 15
- (310) $\leftarrow A \rightarrow$ (004) Ref. 33 or (320) $\leftarrow A \rightarrow$ (014) $\delta v = 8$ Ref. 17
- (310) $\leftarrow C \rightarrow$ (103) Ref. 33 or (320) $\leftarrow C \rightarrow$ (113) $\delta v = 6$ Ref. 17
- (005) $\leftarrow A \rightarrow$ (311) $\delta v = 8$ Ref. 16
- (123) $\leftarrow C \rightarrow$ (330) $\delta v = 6$ Ref. 36
- (401) $\leftarrow C \rightarrow$ (024) $\delta v = 9$ Ref. 36
- (311) $\leftarrow C \rightarrow$ (104) $\delta v = 6$ Ref. 16

Let us note two trends following from the analysis of the above data.

(A) Local resonances involve vibrational states $(v_1 v_2 v_3)$ and $(v'_1 v'_2 v'_3)$ with more and more important difference in vibrational quantum numbers $\delta v = \sum_i |v_i - v'_i|$ up to $\delta v = 12$. An example of the

mixing coefficients for the "exotic" resonance³⁷ between the rotational levels of the states (015) and (080) is shown in Fig. 12.

(") The influence of local resonances with large δv due to accidental closeness of vibrational energies becomes increasingly pronounced in the high-frequency region $\nu > 4000 \text{ cm}^{-1}$. In some case their effect can be comparable with perturbations of rotational levels by principal Coriolis and Darling–Dennison resonances of the first and second order. An example of this type of resonance³⁸ between the states (213) and (420) is shown in Fig. 13.

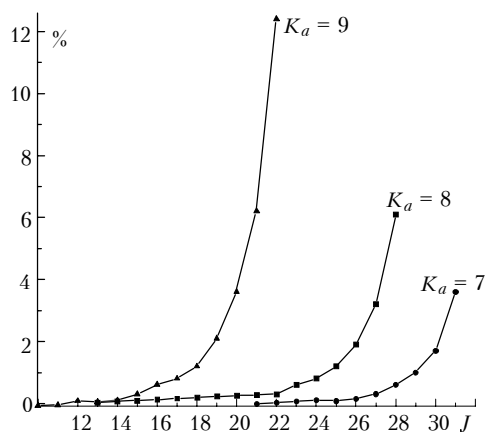


Fig. 12. Mixing coefficients of the rotational–vibrational wavefunctions of the states (015) and (080).

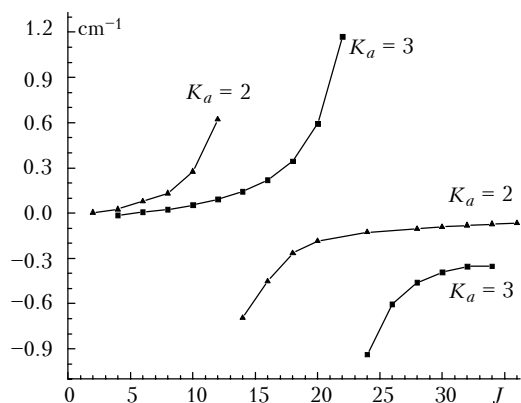


Fig. 13. Resonance perturbations of the rotational levels of the state (213) due to the interaction with the state (420).

On the one hand, these resonances have allowed to obtain important information about "dark" states up to (080) with the vibrational term value estimated $E^{(080)} = 5527.7 \text{ cm}^{-1}$. On the other hand, they clearly

indicate that conventional theory of normal vibrational modes and the standard ordering scheme based on the perturbation theory has a limited applicability at high energy range.

All the above-said concerns the spectra caused by RV transitions within the ground electronic state. The region $9000\text{--}11000 \text{ cm}^{-1}$ is occupied by the ozone absorption bands of another kind. This absorption is formed by the transitions from the ground electronic state to excited electronic states. The study⁴³ reported for the first time an analysis of the rotational structure of a part of this spectrum in the region $9100\text{--}9550 \text{ cm}^{-1}$ and gave spectroscopic parameters and molecular geometry for the state (000) in the 3A_2 electronic state.

In conclusion, we would like to note that the study of high-excited states of the ozone molecule is not of a purely academic interest. In Ref. 44, for example, to describe the ozone emission in the upper atmosphere in the $10\text{--}12.5 \mu\text{m}$ region, the energy levels up to 6350 cm^{-1} with the total vibrational excitation equal to seven are invoked. In the recent review⁴⁵ it is indicated that the knowledge of high-excited states is needed to understand the phenomena of violation of the local thermodynamic equilibrium in the atmosphere. The data on high-excited rotational–vibrational states of ozone are necessary for understanding the dynamics of motion of the nuclei in the ozone molecule and for studying the potential energy surfaces.⁴⁶

Acknowledgments

The authors would like to express their gratitude to Laurence Regalia, Jean-Jacques Plateaux, Xavier Thomas, and Pierre von der Heyden (Reims University, France), Sergei Tashkun and Olga Sulakshina from the Laboratory of Theoretical Spectroscopy of the Institute of Atmospheric Optics S^r RAS (Tomsk, Russia) for many-year fruitful co-operation in the research on ozone spectra. The authors are indebted to Jean-Marie Flaud and Claude Camy-Peyret (CNRS, Paris University) for joint research and stimulating discussions.

This work was done under the financial support from the Russian Foundation for "asic Research, Grant No. 99–03–33201. S. Mikhailenko acknowledges the Ministry of Education and Scientific Research (MESR) of France for the research stipend for 1994–1997. For many years the investigation on IR spectra of ozone was supported by the National Center for Scientific Research (CNRS), IASI CNES, PNCA (France) and the Program of Russian–France Co-operation CNRS-RF" R PICS No. 98–05–22021.

References

1. S.V. Ivanov and V.Ya. Panchenko, *Usp. Fiz. Nauk* **164**, No. 7, 725–742 (1994).
2. I.M. Sizova, *Atmos. Oceanic Opt.* **6**, No. 5, 301–312 (1993).
3. A. Goldman, J.R. Gillis, D.G. Murcray, A. Barbe, and C. Secroun, *J. Mol. Spectrosc.* **96**, No. 2, 279–287 (1982).

4. J.M. Flaud, C. Camy-Peyret, V. Malathy Devi, C.P. Rinsland, and M.A.H. Smith, *J. Mol. Spectrosc.* **124**, No. 1, 209–217 (1987).
5. V. Malathy Devi, J.M. Flaud, C. Camy-Peyret, C.P. Rinsland, and M.A.H. Smith, *J. Mol. Spectrosc.* **125**, No. 1, 174–183 (1987).
6. C.P. Rinsland, M.A.H. Smith, J.M. Flaud, C. Camy-Peyret, and V. Malathy Devi, *J. Mol. Spectrosc.* **130**, No. 1, 204–212 (1988).
7. J.M. Flaud, C. Camy-Peyret, C.P. Rinsland, M.A.H. Smith, and V. Malathy Devi, *J. Mol. Spectrosc.* **134**, No. 1, 106–112 (1989).
8. M.A.H. Smith, C.P. Rinsland, J.M. Flaud, C. Camy-Peyret, and A. Barbe, *J. Mol. Spectrosc.* **139**, No. 1, 171–181 (1990).
9. C. Camy-Peyret, J.M. Flaud, M.A.H. Smith, C.P. Rinsland, V. Malathy Devi, J.J. Plateaux, and A. Barbe, *J. Mol. Spectrosc.* **141**, No. 1, 134–144 (1990).
10. A. Barbe, O. Sulakshina, J.J. Plateaux, A. Hamdouni, and S. Bouazza, *J. Mol. Spectrosc.* **170**, No. 2, 244–250 (1995).
11. A. Barbe, O. Sulakshina, J.J. Plateaux, V.I.G. Tyuterev, and S. Bouazza, *J. Mol. Spectrosc.* **175**, No. 2, 296–302 (1996).
12. A. Barbe, S. Mikhailenko, J.J. Plateaux, and V.I.G. Tyuterev, *J. Mol. Spectrosc.* **182**, No. 2, 333–341 (1997).
13. A. Barbe, J.J. Plateaux, V.I.G. Tyuterev, and S. Mikhailenko, *J. Quant. Spectrosc. Radiat. Transfer* **59**, Nos. 3–5, 185–194 (1998).
14. A. Perrin, A.M. Vasserot, J.M. Flaud, C. Camy-Peyret, V. Malathy Devi, M.A.H. Smith, C.P. Rinsland, A. Barbe, S. Bouazza, and J.J. Plateaux, *J. Mol. Spectrosc.* **149**, No. 3, 519–529 (1991).
15. A. Barbe, S. Bouazza, J.J. Plateaux, and M. Jacon, *J. Mol. Spectrosc.* **162**, No. 2, 335–341 (1993).
16. J.M. Flaud, A. Barbe, C. Camy-Peyret, and J.J. Plateaux, *J. Mol. Spectrosc.* **177**, No. 1, 34–39 (1996).
17. S. Mikhailenko, A. Barbe, V.I.G. Tyuterev, L. Regalia, and J.J. Plateaux, *J. Mol. Spectrosc.* **180**, No. 2, 227–235 (1996).
18. G. Herzberg, *Vibrational and Rotational Spectra of Polyatomic Molecules* [Russian translation] (Izd. Inostr. Lit., Moscow, 1949), 648 pp.
19. J.M. Flaud, C. Camy-Peyret, C.P. Rinsland, M.A.H. Smith, and V.M. Devi, *Atlas of Ozone Spectral Parameters from Microwave to Medium Infrared* (Academic Press, Boston, 1990), 600 pp.
20. N. Jacquinet-Husson et al., *J. Quant. Spectrosc. Radiat. Transfer* **62**, No. 1, 205–254 (1999).
21. L.S. Rothman et al., HITRAN–98. CD ROM.
22. J.J. Plateaux, A. Barbe, and A. Delahaigue, *Spectrochimica Acta Part A* **51**, 1153–1169 (1995).
23. A. Barbe, A. Chichery, V.I.G. Tyuterev, S. Tashkun, and S. Mikhailenko, *Spectrochimica Acta Part A* **54**, 1935–1945 (1998).
24. A. Chichery, V.I.G. Tyuterev, A. Barbe, O. Sulakshina, and Yu. Borkov, *J. Mol. Structure* (1999), in press.
25. S. Mikhailenko, A. Barbe, J.J. Plateaux, and V.I.G. Tyuterev, *J. Mol. Spectrosc.* **196**, No. 1, 93–102 (1999).
26. A. Barbe, S. Mikhailenko, and J.J. Plateaux, *J. Mol. Spectrosc.* **184**, No. 2, 448–453 (1997).
27. S. Bouazza, A. Barbe, S. Mikhailenko, and J.J. Plateaux, *J. Mol. Spectrosc.* **166**, No. 2, 365–371 (1994).
28. A. Barbe and J.J. Plateaux, *J. Quant. Spectrosc. Radiat. Transfer* **55**, No. 4, 449–455 (1996).
29. A. Barbe, S. Mikhailenko, J.J. Plateaux, and V.I.G. Tyuterev, *J. Mol. Spectrosc.* **187**, No. 1, 70–74 (1998).
30. S. Bouazza, A. Barbe, J.J. Plateaux, J.M. Flaud, and C. Camy-Peyret, *J. Mol. Spectrosc.* **160**, No. 2, 371–377 (1993).
31. V. Malathy Devi, A. Perrin, J.M. Flaud, C. Camy-Peyret, C.P. Rinsland, and M.A.H. Smith, *J. Mol. Spectrosc.* **143**, No. 2, 381–388 (1990).
32. S. Bouazza, S. Mikhailenko, A. Barbe, L. Regalia, V.I.G. Tyuterev, and J.J. Plateaux, *J. Mol. Spectrosc.* **174**, No. 3, 510–519 (1995).
33. J.M. Flaud, C. Camy-Peyret, A. Perrin, V. Malathy Devi, A. Barbe, S. Bouazza, J.J. Plateaux, C.P. Rinsland, M.A.H. Smith, and A. Goldman, *J. Mol. Spectrosc.* **160**, No. 2, 378–386 (1993).
34. S. Bouazza, A. Barbe, and J.J. Plateaux, *J. Mol. Spectrosc.* **171**, No. 1, 86–90 (1995).
35. A. Barbe, S. Mikhailenko, V.I.G. Tyuterev, A. Hamdouni, and J.J. Plateaux, *J. Mol. Spectrosc.* **171**, No. 2, 583–588 (1995).
36. A. Barbe, S. Mikhailenko, J.J. Plateaux, and V.I.G. Tyuterev, *J. Mol. Spectrosc.* **185**, No. 2, 408–416 (1997).
37. A. Barbe, A. Chichery, V.I.G. Tyuterev, S. Tashkun, and S. Mikhailenko, *J. Phys. B: At. Mol. Opt. Phys.* **31**, 2559–2569 (1998).
38. A. Barbe and A. Chichery, *J. Mol. Spectrosc.* **192**, No. 1, 102–110 (1998).
39. A. Chichery, A. Barbe, V.I.G. Tyuterev, and J.J. Plateaux, *Molecular Physics* **94**, No. 5, 751–757 (1998).
40. M. Birk, G. Wagner, and J.M. Flaud, *J. Mol. Spectrosc.* **163**, No. 2, 245–261 (1994).
41. M. Birk, G. Wagner, J.M. Flaud, and D. Hausmann, *J. Mol. Spectrosc.* **163**, No. 2, 262–275 (1994).
42. A. Barbe, J.J. Plateaux, S. Bouazza, O. Sulakshina, S. Mikhailenko, V.I.G. Tyuterev, and S. Tashkun, *J. Quant. Spectrosc. Radiat. Transfer* **52**, Nos. 3–4, 341–355 (1994).
43. A.J. Bouvier, D. Inard, V. Veyret, B. Bussery, R. Bacis, S. Churassy, J. Brion, J. Malicet., and R.H. Judge, *J. Mol. Spectrosc.* **190**, No. 2, 189–197 (1998).
44. S.M. Adler-Golden and D.R. Smith, *Planet. Space Sci.* **38**, No. 9, 1121–1132 (1990).
45. J.M. Flaud and R. Bacis, *Spectrochimica Acta Part A* **54**, 3–16 (1998).
46. V.I.G. Tyuterev, S. Tashkun, P. Jensen, A. Barbe, T. Cours, *J. Mol. Spectrosc.* **198**, 57–76 (1999).